Ad Hoc Networks 51 (2016) 1–10

Contents lists available at ScienceDirect

Ad Hoc Networks

journal homepage: www.elsevier.com/locate/adhoc

Gaussian Process Regression for Fingerprinting based Localization

Sudhir Kumar[a], Rajesh M. Hegde[a,*], Niki Trigoni[b]

[a] Department of Electrical Engineering, Indian Institute of Technology, Kanpur, India
[b] Department of Computer Science, University of Oxford, United Kingdom

ARTICLE INFO

Article history:
Received 9 February 2016
Revised 2 July 2016
Accepted 18 July 2016
Available online 25 July 2016

Keywords:
Localization
Gaussian process regression
Cramér-Rao bound

ABSTRACT

In this paper, Gaussian process regression (GPR) for fingerprinting based localization is presented. In contrast to general regression techniques, the GPR not only infers the posterior received signal strength (RSS) mean but also the variance at each fingerprint location. The GPR does take into account the variance of input i.e., noisy RSS data. The hyper-parameters of GPR are estimated using trust-region-reflective algorithm. The Cramér-Rao bound is analysed to highlight the performance of the parameter estimator. The posterior mean and variance of RSS data is utilized in fingerprinting based localization. The principal component analysis is employed to choose the k strongest wi-fi access points (APs). The performance of the proposed algorithm is validated using using real field deployments. Accuracy improvements of 10% and 30% are observed in two sites compared to the Horus fingerprinting approach.

1. Introduction

The received signal strength (RSS) based mobile user localization method has recently attracted significant attention. Perhaps this happened because RSS measurements from the wi-fi access points in indoor scenarios provide a cost-effective positioning system. It does not require any additional hardware unlike time of arrival (TOA), time-difference of arrival (TDOA) and angle of arrival (AOA). The time based localization techniques are also limited by the fact that it requires highly precise synchronization. On the other hand, RSS based localization techniques suffer from the harsh wireless channel such as multipath fading, and non-homogeneous environment. Hence, it is of sufficient interest to develop the robust fingerprint method which is relatively stable during different days with high localization accuracy.

Several localization algorithms in literature are based on two steps procedures. In the first step, inter-nodal range is estimated with learning of radio propagation model. Subsequently, these estimated ranges are further utilized in positioning the user. In doing so, large range error propagates into positioning phase. In contrast, fingerprinting based localization methods provide higher accuracy at the expense of extensive training. It may be noted that training is required even for learning radio propagation model to some extent. In this paper, sparse RSS data are collected from the given area of interest. Subsequently, Gaussian process regression (GPR) is employed to build the posterior mean and variance at each of the locations. These predicted variances are further utilized for localization during test phase. The motivation for using Gaussian process in this work stems from the fact that it not only predicts the RSS mean but also infers the variance at each location. The main contributions of the paper are enumerated herein.

1. We present the textbook derivation of Cramér-Rao Lower Bound (CRLB) on estimation error of kernel function hyper-parameters in the context of GPR framework using basic CRLB theory. This helps us in obtaining the minimum variance of the unbiased estimator for given hyper-parameter. We also obtain the required number of snapshots for the good estimate of hyper-parameters using CRLB expression.
2. We show that the localization accuracy with fingerprint constructed using GPR is higher than the Horus fingerprinting approach. Further, localization accuracy is not significantly affected by the reduction in number of samples at each fingerprint location. Accuracy improvements of 10% and 30% are observed in two sites compared to the Horus fingerprinting approach.
3. We further illustrate that localization accuracy is relatively insensitive to the choice of different kernel functions such as Gaussian, Laplacian and Exponential. The performance of Laplacian and Exponential kernel functions is the same because the only difference lies with the length scale parameter.
4. There are plenty of insignificant APs like commuter phone wi-fi, vehicle wi-fi besides fixed APs, in crowded wireless environment, e.g, supermarket. To find out the set of strongest APs in

* Corresponding author.
E-mail addresses: sudhirkr@iitk.ac.in (S. Kumar), rhegde@iitk.ac.in (R.M. Hegde), niki.trigoni@cs.ox.ac.uk (N. Trigoni).

http://dx.doi.org/10.1016/j.adhoc.2016.07.014
1570-8705/

the given area of interest, a criterion based on dimensionality reduction using principal component analysis is employed.

The remainder of the paper is organized as follows: Section 2 overviews existing techniques for localization. Section 3 describes the Gaussian process regression for fingerprinting based localization. Performance evaluation is presented in Section 4. A brief conclusion is presented in Section 5. Cramér-Rao lower bound (CRLB) analysis for the kernel function parameters is discussed in Appendix.

2. Background

In this section, various kind of localization techniques are reviewed: 1) indoor positioning based on propagation model; 2) multi-sensor data fusion based method; 3) fingerprinting based methods, and 4) regression based methods.

2.1. Indoor Positioning Based on Radio Propagation Model

The localization methods based on propagation model [1–4] are generally two step procedures. First the inter-nodal range is estimated. Subsequently, these estimated ranges are utilized for positioning with the set of APs coordinates. The path-loss model [2] increases exponentially with range. The break point path loss model (also called dual slope model) [3] to account for different path loss in two breakpoint regions. The wall and floor attenuation factors are considered in COST231-MWM model [4]. Estimated range using these propagation models is highly erroneous. The error is in the range of 7 m - 8 m for our considered experimental scenario. This is because the propagation model assumes wi-fi signal strength due to a particular AP decreases with the distance isotropically. However, it is not true because of non-homogeneous environment. Finally, these errors further propagate into the positioning phase and make the indoor positioning system highly inaccurate.

2.2. Multi-Sensor Data Fusion Based Localization

In order to enhance the accuracy of a localization system, we may resort to fusion based approach. Wi-fi based SLAM [5–8] fuses RSS and motion sensor data for simultaneous building a map and locating a user. The RAVEL, radio and vision enhanced localization system, which fuses wi-fi with visual data is explored in [9]. Further, the organic landmark maps utilize the unique identifiable signatures within the building [10,11]. These signatures then correct the dead-reckoning error for enhanced accuracy in this unsupervised localization method.

2.3. Fingerprinting Based Localization

Standard fingerprinting based localization methods available in the literature are RADAR [12], PlaceLab [13], and Horus [14]. These methods comprise primarily two phase: training and testing. During training phase, radio map is generated at each of the fingerprint location. Subsequently, a location is chosen corresponding to the minimum error between test RSS data and fingerprint RSS. [15,16] are presented to cope up with heterogeneous devices during training and testing phase. [15] utilizes ratio of RSS, whereas, [16] uses relative RSS data and performance deteriorates [17].

The channel state information (CSI) utilizes physical layer information to deal with the multipath fading effect and it performs better than RSS based methods under certain conditions [18]. Choosing the location dependent, temporally stable, and noise resilient feature is a challenging task in both CSI and RSS framework [18]. Fingerprinting database is built and updated in both CSI and RSS framework which is labour-intensive and time-consuming [19]. CSI based method is also constrained by the underlying bandwidth. Additionally, CSI based methods, in particular, require additional hardware to estimate the angle of arrival of multipath components [20] or time of flight information from physical layer [21] or wifi network interface cards (NIC) or 802.11a/g/n wireless connection [22,23]. On the contrary, RSS measurements are accessible on mobile phones in wireless techniques ranging from ZigBee, UWB and WiFi to cellular networks [18]. It can be easily measured using hand-held devices, e.g., mobile phone, smart watch and tablet from fixed APs without any modification in the existing hardware [22,24].

Notably, fingerprinting based localization methods provide good location accuracy at the expense of heavy training during radio map construction. In order to reduce the calibration efforts, crowdsourcing for localization is explored in [8,11,22,25–29]. However, these methods provide coarse location resolution.

2.4. Regression Based Localization

General regression or interpolation based approaches such as polynomial fitting [30], exponential fitting, and log model are limited by the fact that it only predicts the RSS mean not the variance of the estimate. However, for localization using probabilistic based method, we are interested not only in the posterior RSS mean but also how certain that mean is. The polynomial models have poor interpolatory, and asymptotic properties and it is also difficult to extrapolate outside the range of observations. The exponential regression is suitable for line-of-sight (LOS) scenario. It may be noted that variants of the log based regression are explained above in Section 2.1.

The Gaussian process regression for sensor networks under localization uncertainty is proposed in [31]. The Monte Carlo sampling and Laplace approximation are used to compute analytically intractable posterior distribution. Notably, this method does not consider the location estimation problem using Gaussian process. The Gaussian process inference approximation using multi-sensor data such as inertial, magnetic, signal strength and time-of-flight measurements for indoor pedestrian localization is discussed in [32]. [33] considers the near-optimal sensors placement problem using mutual information in this context. The wi-fi SLAM using Gaussian process latent variable models is presented in [5]. Gaussian process assisted fingerprinting localization is discussed in [34]. In this work, user's location is obtained through exhaustive search of likelihood function. Moreover, this is a discrete location estimator. Learning-based indoor localization using Gaussian processes is described in [35]. The method used to train hyper-parameters is not clearly mentioned [34,35].

In summary, all the localization algorithms either use radio propagation model, multi-sensor data fusion, training based fingerprinting or regression based localization. The multi-sensor data fusion based localization utilizes rich sensors for good accuracy. It may lead to high cost at implementation stage. Localization based on radio propagation model is inaccurate, whereas, fingerprinting localization yields good accuracy at the expense of extensive training. In this paper, the proposed method is semi-supervised due to the fact that RSS measurements are collected sparsely across the indoor area and subsequently entire fingerprinting database is constructed for localization. This extends the applicability of the proposed method for practical situations. It may be noted that indoor multipath reflections and shadowing problem can be mitigated upto a large extent by employing a large number of existing APs. Although, Gaussian process has been widely used in the sensor networks. However, none of the methods consider the problem to obtain the CRLB of the kernel function hyper-parameters and this was an open problem, to the author's best knowledge. This is

especially relevant to know the sensitivity of the hyper-parameters estimation on the localization error.

3. GPR for Fingerprinting based Localization

In this section, first the introduction to Gaussian process regression is presented, as in [36,37]. Kernel parameters estimation using gradient based method is then detailed. Subsequently, Cramér-Rao lower bound analysis and fingerprinting based localization are followed.

3.1. Gaussian Process Regression

A Gaussian process is a stochastic process, and any finite number of collections follow a joint Gaussian distribution [36]. Consider the following observation model.

$$y = f(\mathbf{x}) + \eta \tag{1}$$

where η represents the i.i.d. (independent, identically distributed) Gaussian noise with zero mean and variance, σ_n^2, i.e., $\eta \sim \mathcal{N}(0, \sigma_n^2)$. In this work, letters in bold (upper or lower) denote matrix. It may be noted that y denotes the observations which is wi-fi signal strength at particular location. $\mathbf{x}$ is the input features, i.e., location coordinates.

The mean function, $m(\mathbf{x})$, and covariance function, $k(\mathbf{x}_i, \mathbf{x}_j)$, for latent function, f, can be stated as

$$m(\mathbf{x}) = \mathbb{E}[f(\mathbf{x})] \tag{2}$$

$$k(\mathbf{x}_i, \mathbf{x}_j) = \mathbb{E}[(f(\mathbf{x}_i) - m(\mathbf{x}_i))(f(\mathbf{x}_j) - m(\mathbf{x}_j))] \tag{3}$$

where $\mathbb{E}(.)$ denotes the expectation operator. Without loss of generality, mean can be considered as zero. The kernel function considered in this work is expressed as

$$k(\mathbf{x}_i, \mathbf{x}_j) = \sigma_f^2 \exp\left(-\frac{||\mathbf{x}_i - \mathbf{x}_j||}{2l^2}\right) \tag{4}$$

where σ_f^2 and l are called the hyper-parameters. σ_f^2 denotes the signal variance, while l the length scale parameter, which characterizes the smoothness of a function. $\mathcal{L}_2$ norm is represented by ||.||, which denotes the Euclidean distance between two vectors. The Gramian matrix, $\tilde{\mathbf{K}}$, is defined using Equation 4 as

$$\tilde{\mathbf{K}} = \begin{bmatrix} k(\mathbf{x}_1, \mathbf{x}_1) & k(\mathbf{x}_1, \mathbf{x}_2) & \dots & k(\mathbf{x}_1, \mathbf{x}_N) \\ k(\mathbf{x}_2, \mathbf{x}_1) & k(\mathbf{x}_2, \mathbf{x}_2) & \dots & k(\mathbf{x}_2, \mathbf{x}_N) \\ \vdots & \vdots & \ddots & \vdots \\ k(\mathbf{x}_N, \mathbf{x}_1) & k(\mathbf{x}_N, \mathbf{x}_2) & \dots & k(\mathbf{x}_N, \mathbf{x}_N) \end{bmatrix} \tag{5}$$

where the total number of fingerprint locations is denoted by N. Thus, $f(\mathbf{x})$ can be stated as Gaussian process.

$$f(\mathbf{x}) \sim \mathcal{GP}(m(\mathbf{x}), k(\mathbf{x}_i, \mathbf{x}_j)) \tag{6}$$

where latent function, f is characterized using Gaussian process with mean function, $m(\mathbf{x})$, and covariance function, $k(\mathbf{x}_i, \mathbf{x}_j)$.

The training $\mathbf{y}$ and test y_* wi-fi data can follow multivariate Gaussian distribution jointly as

$$\begin{bmatrix} \mathbf{y} \\ y_* \end{bmatrix} \sim \mathcal{N}\left(\mathbf{0}, \begin{bmatrix} \tilde{\mathbf{K}}(\mathbf{X}, \mathbf{X})_{N\times N} & \tilde{\mathbf{K}}(\mathbf{X}, \mathbf{X}_*)_{N\times N_*} \\ \tilde{\mathbf{K}}(\mathbf{X}_*, \mathbf{X})_{N_*\times N} & \tilde{\mathbf{K}}(\mathbf{X}_*, \mathbf{X}_*)_{N_*\times N_*} \end{bmatrix}\right) \tag{7}$$

where suffix of the block covariance matrix denotes the size of that particular matrix, for N training wi-fi data and N_* test data. The posterior distribution, $p(y_*|\mathbf{y})$, which signifies how likely is a prediction y_*, given the data $\mathbf{y}$ is

$$\begin{aligned} y_*|\mathbf{y} \sim \mathcal{N}\big(&\tilde{\mathbf{K}}(\mathbf{X}_*, \mathbf{X})\tilde{\mathbf{K}}(\mathbf{X}, \mathbf{X})^{-1}\mathbf{y}, \\ &\tilde{\mathbf{K}}(\mathbf{X}_*, \mathbf{X}_*) - \tilde{\mathbf{K}}(\mathbf{X}_*, \mathbf{X})\tilde{\mathbf{K}}(\mathbf{X}, \mathbf{X})^{-1}\tilde{\mathbf{K}}(\mathbf{X}, \mathbf{X}_*)\big) \end{aligned} \tag{8}$$

Thus, posterior RSS mean and variance at each fingerprint location can be computed. In order to estimate these, we require the kernel function hyper-parameters which is described in the ensuing subsection.

3.2. GPR Parameters Estimation

Generally, we have noisy wi-fi signal observations at each of the fingerprint locations. The Gaussian process allow us to include variance of the noise, σ_n^2, present in the wi-fi data. First, Gaussian process learns the hyper-parameters using optimization technique from noisy wi-fi data. The optimization technique utilized in this work is subspace trust-region method which is based on interior-reflective Newton method [37–39]. It minimizes a non linear function subject to simple bounds. Since the hyper-parameters need to be positive, we set a large positive number as an upper bound, whereas zero as a lower bound. Ten initial guess of hyper-parameters are chosen uniformly within this lower and upper bound, and then optimization is carried out. The parameters which maximize the marginal log-likelihood function is finally opted as a solution of this problem. Additionally, gradient of the optimization problem is easy to compute because of the continuity and differentiability properties. It may be noted that we have also increased the number of initial guess, typically 10 to 1000 and upper bound, typically 1 to 1000, and found that parameters which maximize the marginal log-likelihood function is insensitive to it.

Subsequently, we compute posterior RSS mean and variance at each locations in the building using these estimated hyper-parameters. We have explained herein an optimization approach to estimate the hyper-parameters. In order to know that how well the estimated parameters is, we need minimum variance of the estimated parameters. For this, Cramér-Rao bound analysis is presented in ensuing subsection and appendix.

3.3. Cramér-Rao Lower Bound Analysis

Cramér-Rao bound [40,41] provides the lower bound on the variance of any unbiased estimator. It is the standard benchmark with respect to which, variance of any estimator is compared. Hence, it is of sufficient interest to develop an expression for Cramér-Rao bound for the kernel function parameters.

The variance of any unbiased estimator $\hat{\theta}$ of $\boldsymbol{\theta}$ is lower bounded by the inverse-fisher information, $\mathbf{I}^{-1}(\theta)$. The FIM is the amount of information that an wi-fi observation $\mathbf{y}$ contains about unknown parameters, $\boldsymbol{\theta} = \begin{bmatrix} l & \sigma_f \end{bmatrix}^{\mathrm{T}}$, where $(.)^{\mathrm{T}}$ represents the transpose of a matrix. It measures on an average how peaked the likelihood function will be for an observation $\mathbf{y}$, given parameter $\boldsymbol{\theta}$. It can be also interpreted as how much curvature the likelihood function will have at maximum. If it is peaked around maximum, it will have lower variance and consequently more information.

In order to develop the CRLB for unknown parameter $\boldsymbol{\theta}$, we first need to derive log-likelihood function of a $\boldsymbol{\theta}$, given an wi-fi observation $\mathbf{y}$. Subsequently, FIM is computed, having verified the regularity condition. Finally, the square root of trace of a inverse-FIM is evaluated for CRLB. For the sake of simplicity and shortness, the Cramér-Rao bound analysis is presented in Appendix.

3.4. Fingerprinting based Localization

Each of the fingerprint location in the given area of interest is assigned a probability. This is computed as probability of a fingerprint location, $\mathbf{z}_n$, given the wi-fi signal observation vector, $\mathbf{S}$. According to Bayes theorem, $p(\mathbf{z}_n|\mathbf{S})$ can be expressed in terms of $p(\mathbf{S}|\mathbf{z}_n)$. The unknown location estimate can be expressed as the

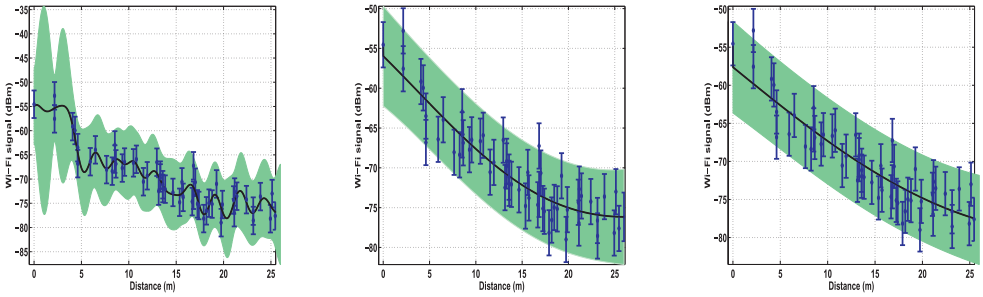

(a) $(l, \sigma_f) = (1, 16.08)$, LE = 3.04 m (b) $(l, \sigma_f) = (21.18, 16.08)$, LE = 2.41 m (c) $(l, \sigma_f) = (40, 16.08)$, LE = 2.77 m

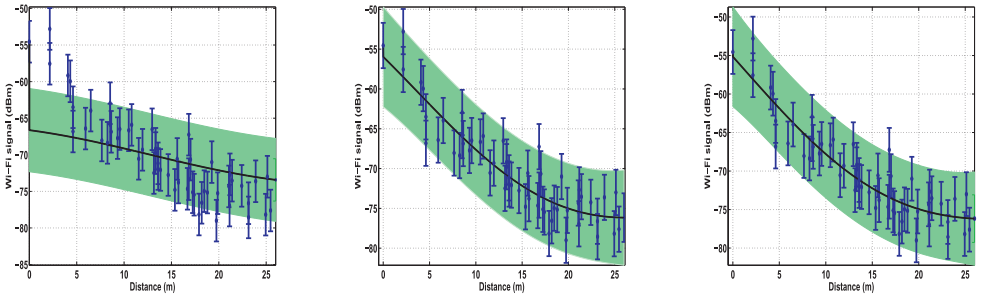

(d) $(l, \sigma_f) = (21.18, 1)$, LE = 8.60 m (e) $(l, \sigma_f) = (21.18, 16.08)$, LE = 2.41 m (f) $(l, \sigma_f) = (21.18, 30)$, LE = 2.46 m

Fig. 1. Figure illustrating the posterior RSS mean (in black curve) and confidence interval (in shaded green). Real wi-fi data are shown in Blue.

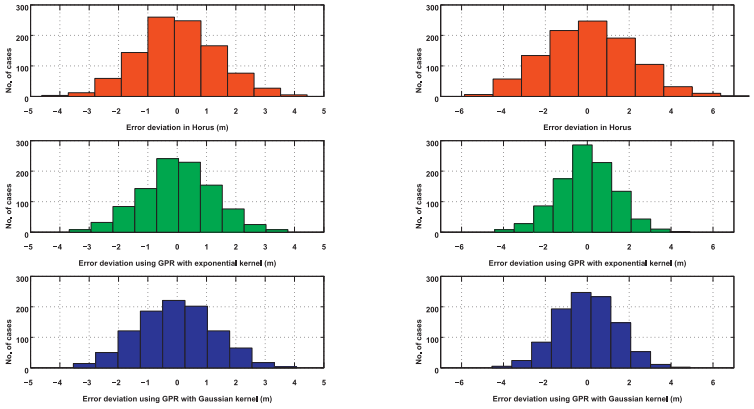

(a) Academic area (b) Supermarket

Fig. 2. Figure illustrating the insensitivity of kernels over localization accuracy.

weighted sum of probabilities.

$$\hat{\mathbf{z}} = \frac{\sum_{i=n}^{N} \mathbf{z}_n p(\mathbf{S}|\mathbf{z}_n)}{\sum_{n=1}^{N} p(\mathbf{S}|\mathbf{z}_n)} \tag{9}$$

where $\mathbf{z}_n = [x_n \;\; y_n]^{\mathrm{T}}$ represents the n^{th} fingerprinting location, $n \in \{1, 2, \ldots, N\}$. S denotes the wi-fi signal observation vector at each of the fingerprinting location. The total number of APs is represented by A and $A << N$. The $p(\mathbf{S}|\mathbf{z}_n)$ can be computed, assuming the independence between all APs as

$$p(\mathbf{S}|\mathbf{z}_n) = \prod_{a=1}^{A} \frac{1}{\sqrt{2\pi\,\Sigma_n(a,a)}} \exp\left(-\frac{(s_a - \mu_a)^2}{2\Sigma_n(a,a)}\right) \tag{10}$$

It may be noted that localization is carried out in two-dimensional coordinate system herein, however, extension to three dimensions is straightforward.

4. Performance Evaluation

In this section, first the experimental conditions for localization in two different scenarios are presented. Subsequently, experimental results for fingerprinting based localization are detailed.

4.1. Experimental Conditions

The extensive experiments are conducted in two different environmental conditions such as academic area of a university and supermarket.

4.1.1. Academic Area

Figure 7(a) shows the floor plan of third floor of Wolfson building, University of Oxford. The four APs (TP-Link, TL-WA901ND) are manually deployed as shown in figure. The wi-fi data are collected for five different days at each of the fingerprint locations using Moto-E android mobile phone. The wi-fi signal for fifth day is chosen to build the fingerprint database, whereas wi-fi data of other days are for online test data. Measurements are recorded at total twenty eight locations on a closed path for duration of approximately ten seconds at each. Approximately ten wi-fi samples are captured in this given durations at each location, however, sampling rate depends upon the hardware of mobile phone being used. We present the localization results for two days only. Notably, similar results are obtained for other days in this scenario. The similar results are seen for fourth floor of this building too.

4.1.2. Supermarket

The experiments are conducted in another environmental conditions like supermarket as shown in Figure 7(b). The slab between fingerprint locations is basically the shelf for grocery items. People movements in supermarket are far more than the academic area which impact the localization performance. Similar to our academic area experimental set-up, wi-fi data are collected at 56 locations using android mobile phone for duration of 10 seconds at each location. The total 23 APs are noticed in the basement of this market. There are numerous insignificant APs such as commuter phone wi-fi, and vehicle wi-fi. Some of the wi-fis are static and many of them are mobile. There is not any reasonable improvement in localization accuracy with utilization of the weakest APs. This also makes sense because we need same set of static APs over training and testing phase for different days. To find out the set of strongest APs in the given area of interest, a criterion based on dimensionality reduction using principal component analysis is employed as following.

Let $\mathbf{S}$ be the signal observation matrix of dimension $N \times A$. The eigen values of the signal covariance matrix $[\mathbf{S}^T\mathbf{S}]$ is denoted by λ_a, $\forall\ a = \{1, 2, \ldots, A\}$. The objective is find minimum $\bar{A}$ such that following criteria is met.

$$\mathcal{T} = \frac{\sum_{a=1}^{\bar{A}} \lambda_a}{\sum_{a=1}^{A} \lambda_a} \geq 99.9 \tag{11}$$

In this work, 99.9% variance criterion is retained to choose the 9 strongest APs out of total 23 APs. Note that, different variance threshold may be opted depending upon the applications specific requirements. It may be noted here that we were not intended to know the APs location, neither we had any privilege to the placement of these APs.

4.2. Experimental Results

In this section, first impact of hyper-parameters and insensitivity to different closely related kernels on the localization error performance are followed next. Subsequently, average localization error and trajectory analysis in two different scenarios are presented.

4.2.1. Cramér-Rao Lower Bound Analysis

In order to assess minimum variance of the parameter estimate, CRLB analysis is described in Figure 3. It can be seen that the RMSE of the hyper-parameters attains the derived CRLB and achieves an asymptotically efficient performance. Forty snap-shots are sufficient for good estimate of hyper-parameters as in Figure 3.

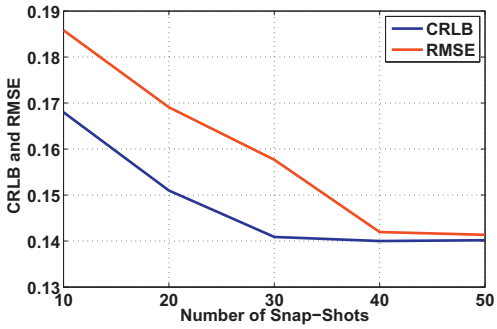

Fig. 3. Variation of CRLB and RMSE with number of wi-fi signal snap-shots.

4.2.2. Significance of Hyper-parameters Estimation

Figure 1 depicts the impact of hyper-parameter estimation on the posterior RSS mean and variance. It eventually impacts the localization performance. Posterior RSS mean and variance using optimal hyper-parameters is shown in Figure 1(b) and 1(e). Note that Figure 1(b) and Figure 1(e) are same and it is just for the symmetric placement of figures. Figure 1(a) and Figure 1(c) denote the localization performance using lower ($l = 1$) and larger ($l = 40$) length scale values respectively, keeping σ_f fixed. In fact, length scale characterizes how smooth our predicted mean is. If l is lower, we can distinguish neighbouring location i.e., high resolution. On the other hand, larger l signifies slower variation in predicted RSS mean at neighbouring locations and hence lower resolution. Although, lower l has higher resolution, but it can have poor interpolatory and extrapolatory capability. It may provide low RSS training error but may have significant test error.

Additionally, σ_f^2 denotes the wi-fi signal variance. This measures the variation of RSS prediction from the mean. Smaller the σ_f^2, slower the variation of the function, and high similarity at neighbouring location and vice-versa. Therefore, optimal hyper-parameters are required for the given scenario.

4.2.3. Illustration of Insensitivity of Different Kernels

Figure 2 depicts the impact of different closely related kernels on the performance of average localization error deviation. Gaussian, Exponential and Laplacian kernels are utilized for the same and compared it with standard fingerprinting based Horus localization method. The localization error with the use of Exponential and Laplacian kernels are same because the only difference lies with the length scale parameter. Localization performance using Exponential kernel performs slightly better than Gaussian kernel. Notably, our proposed fingerprinting based GPR with these kernels performs better than Horus method.

4.2.4. Impact of Number of APs on Localization Error

The localization error with confidence intervals is shown in Figure 4 for two scenarios. The fifth day is chosen for training the GPR, while day 1 and day 2 are utilized for test sites. The localization performance in academic area is better than supermarket as expected and reason mentioned above. The result using GPR is relatively better in supermarket than academic area. Since, Horus uses time averaged RSS for training and test database. Therefore, time average RSS tends to deteriorate relatively higher than predicted (or smoothed) RSS, in crowded place. It may be noted that similar localization results are found if we change the order of training and test days.

4.2.5. Impact of Fingerprint Locations on Localization Error

Figure 5 depicts the impact of varying fraction of total fingerprinting location on the average localization error. This much fraction of fingerprint locations are utilized in weighted sum of

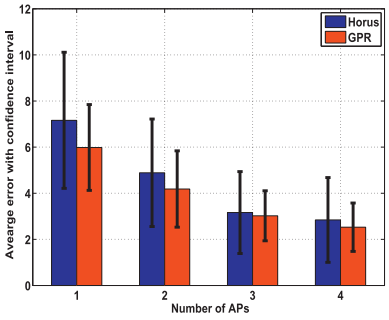

(a) Academic area: Day 1

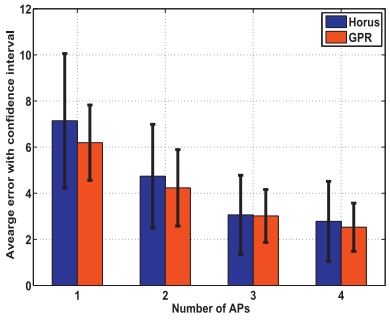

(b) Academic area: Day 2

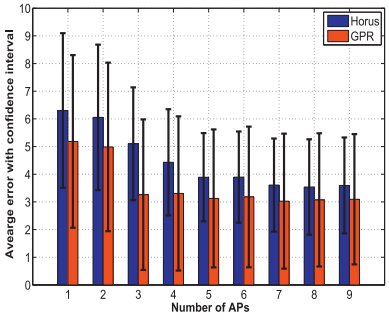

(c) Supermarket: Day 1

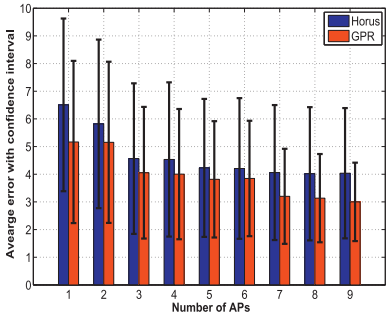

(d) Supermarket: Day 2

Fig. 4. Figure illustrating the average localization error (m) and confidence interval for two sites.

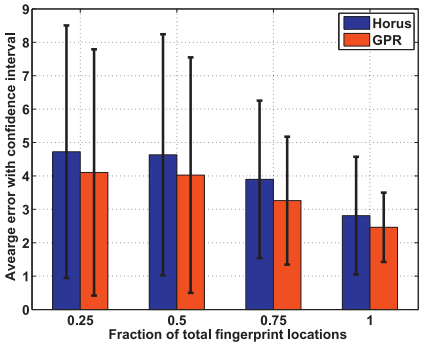

(a) Academic area: Day 1

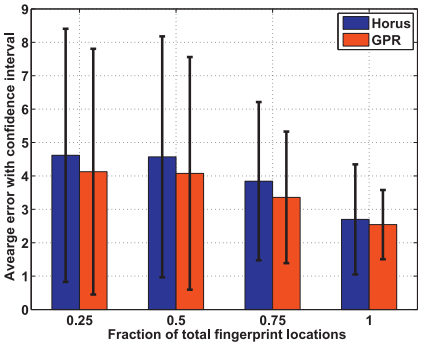

(b) Academic area: Day 2

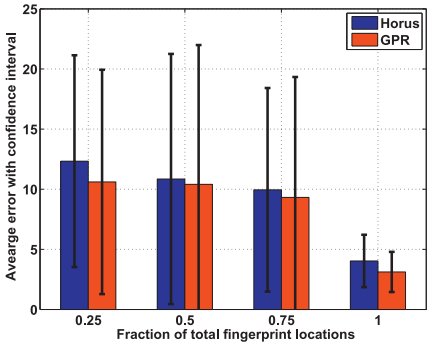

(c) Supermarket: Day 1

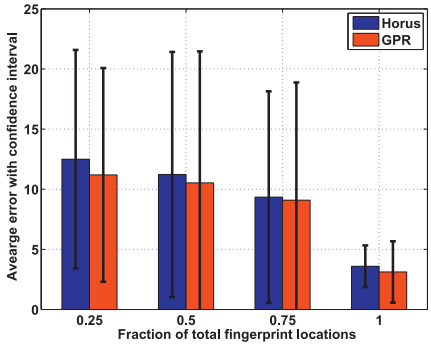

(d) Supermarket: Day 2

Fig. 5. Figure illustrating the average localization error (m) and confidence interval with varying fraction of total fingerprint locations in weighted average.

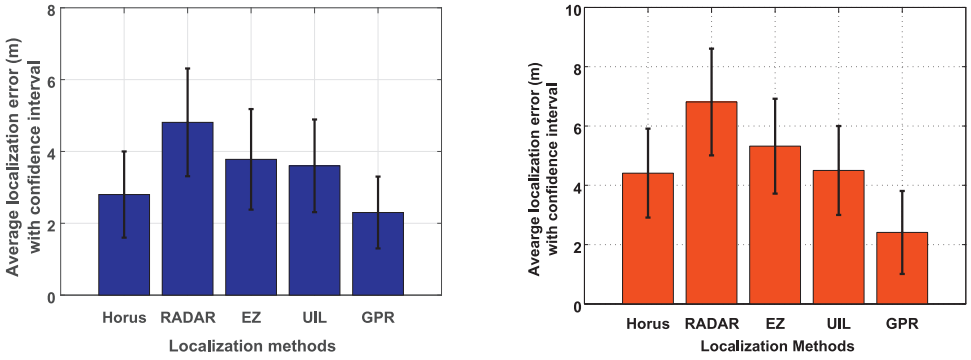

(a) (b)

Fig. 6. Figure illustrating the comparison of localization error for different methods in two sites.

(a) Academic area, LE: (Horus, GPR) = (2.8 m, 2.3 m)

(b) Supermarket, LE: (Horus, GPR) = (4.03 m, 2.41 m)

Fig. 7. Illustrative examples showing the effectiveness of the proposed algorithm with respect to Horus in two sites.

probabilities for location estimation. As the fraction of fingerprinting locations increases, average localization error goes down. Considering a large number of fingerprinting locations improves the localization accuracy on an average sense. Average localization error reduces approximately from 5 m and 12 m to 3 m in academic area and supermarket respectively.

4.2.6. Comparison of Average Localization Errors

We illustrate the effectiveness of the proposed GPR method in comparison with RADAR [12], HORUS [14], EZ [42], and UIL [43] in Figure 6. The average localization errors in site 1 for HORUS, RADAR, EZ, UIL and GPR methods are 2.8 m, 4.81 m, 3.78 m, 3.6 m, 2.3 m respectively. Similarly, the average localization errors in site 2 for those methods are 4.41 m, 6.81 m, 5.32 m, 4.54 m, 2.41 m respectively. The proposed method outperforms the existing methods in terms of localization error and its standard deviation for both sites.

4.2.7. Trajectory Analysis

In order to know the individual estimated location accuracy, trajectory analysis is shown in Figure 7 for two scenarios. Blue color represents the ground truth, while red and green the estimated location with Horus and GPR method respectively. In Figure 7(a), GPR performs marginally better than Horus because of less people movements. The localization error for GPR is 2.3 m, whereas 2.8 m for Horus. Horus tends to deteriorates in supermarket as shown in Figure 7(b), as expected. The average localization for all locations is 4.03 m and 2.41 m for Horus and GPR method respectively is supermarket. Thus, it can be concluded that GPR based localization method is more effective in harsh environment.

5. Conclusion and Future Work

In this paper, localization accuracy with respect to the standard Horus technique is achieved at the expense of $O(N^3)$ computational complexity. This complexity arises from wi-fi signal prediction at each location using Gaussian process regression (GPR). To further reduce it, network segmentation having complexity $O(N'^3)$, $N' \leq N$, can be employed. Future work includes developing a real-time positioning system that localize as we go, i.e, calibration-free localization.

We collect approximately ten wi-fi signal snap-shots at each location to minimize the effect of small-scale fading. The performance of this localization system will be affected if we collect a very few number of snap-shots. This is because wi-fi signal is not very reliable. In this case, at some locations, corresponding wi-fi signal may be treated as outliers. If the number of such outliers is less than the 50% of the total wi-fi observations at all locations, Gaussian process with Student-t likelihood can be utilized, in this context to deal with outliers. Although, conditional posterior is intractable for this non-Gaussian likelihood, and approximation is required with Markov chain Monte Carlo, Laplace approximation, or expectation propagation algorithm.

The fingerprint location can slightly differ with untrained labours, and it of course affects the localization performance. Therefore, we need to take fingerprint location uncertainty into

account. It can be scattered inside a circle with certain radii, and follow Gaussian or uniform distribution.

Acknowledgment

This work was carried out under Erasmus Mundus - Namaste exchange fellowship program at University of Oxford, United Kingdom. The author S. Kumar was also supported by Tata Consultancy Research (TCS) scholarship program TCS/CS/2011191C. The authors would like to thank the all the current members of the Sensor Networks group for the valuable discussion.

Appendix A

A1. Cramér-Rao Lower Bound (CRLB) Analysis for the Kernel Function Parameters

Let unknown hyper-parameters, $\boldsymbol{\theta} = \begin{bmatrix} l & \sigma_f \end{bmatrix}^{\mathrm{T}}$, where $(.)^{\mathrm{T}}$ represents the transpose of a matrix. The variance of any unbiased estimator $\hat{\theta}$ of $\boldsymbol{\theta}$ is lower bounded by the inverse-fisher information, $\mathbf{I}(\boldsymbol{\theta})$.

$$v^r(\hat{\theta}_j) \geq [\mathbf{I}^{-1}(\boldsymbol{\theta})]_{jj} \tag{12}$$

where $v^r(.)$ denotes the variance operator. The Fisher Information Matrix (FIM) is expressed as

$$\mathbf{I}(\boldsymbol{\theta}) = -\begin{bmatrix} \mathbb{E}\left[\frac{\partial^2 lnp(.)}{\partial l^2}\right] & \mathbb{E}\left[\frac{\partial^2 lnp(.)}{\partial l \partial \sigma_f}\right] \\ \mathbb{E}\left[\frac{\partial^2 lnp(.)}{\partial l \partial \sigma_f}\right] & \mathbb{E}\left[\frac{\partial^2 lnp(.)}{\partial \sigma_f^2}\right] \end{bmatrix} \tag{13}$$

The marginal likelihood in terms of latent function, $\mathbf{f}$, can be written as [36]

$$p(\mathbf{y}|\mathbf{X}) = \int \underbrace{p(\mathbf{y}|\mathbf{f},\mathbf{X})}_{\text{likelihood}} \underbrace{p(\mathbf{f}|\mathbf{X})}_{\text{prior}} d\mathbf{f} \tag{14}$$

The prior is generally assumed to be Gaussian in Gaussian process i.e.,

$$\mathbf{f}|\mathbf{X} \sim \mathcal{N}(\mathbf{0}, \tilde{\mathbf{K}}) \tag{15}$$

Therefore,

$$\log p(\mathbf{f}|\mathbf{X}) = -\frac{1}{2}\mathbf{f}^T\tilde{\mathbf{K}}^{-1}\mathbf{f} - \frac{1}{2}\log|\tilde{\mathbf{K}}| - \frac{N}{2}\log 2\pi \tag{16}$$

where N is the size of a observation vector. The likelihood can be thought as a Gaussian, i.e.,

$$\mathbf{y}|\mathbf{f} \sim \mathcal{N}(\mathbf{f}, \sigma_n^2\mathbf{I}) \tag{17}$$

where $\mathbf{I}$ denotes the identity matrix of appropriate dimensions. Thus, log marginal likelihood in Equation 14 can be recast as

$$\log p(\mathbf{y}|\mathbf{X}) = -\frac{1}{2}\mathbf{y}^T(\tilde{\mathbf{K}} + \sigma_n^2\mathbf{I})^{-1}\mathbf{y} - \frac{1}{2}\log|\tilde{\mathbf{K}} + \sigma_n^2\mathbf{I}| - \frac{N}{2}\log 2\pi \tag{18}$$

In order to compute the FIM, we require double derivative of the log likelihood function with respect to each unknown parameter.

$$\frac{\partial \log p(\mathbf{y}|\mathbf{X})}{\partial \theta_j} = \frac{1}{2}\mathbf{y}^T\mathbf{K}^{-1}\frac{\partial \mathbf{K}}{\partial \theta_j}\mathbf{K}^{-1}\mathbf{y} - \frac{1}{2}\mathrm{tr}\left(\mathbf{K}^{-1}\frac{\partial \mathbf{K}}{\partial \theta_j}\right), \quad \forall j = 1,2 \tag{19}$$

where tr(.) represents the trace of a matrix, which is the sum of diagonal elements. For notational brevity, $[\tilde{\mathbf{K}} + \sigma_n^2\mathbf{I}]$ is represented by $\mathbf{K}$. Notably, likelihood function does satisfy the regularity condition, which is desirable according to CRLB theorem.

$$\mathbb{E}_{\mathbf{y}}\left[\frac{\partial \log p(\mathbf{y}|\mathbf{X})}{\partial \theta_j}\right] = 0 \tag{20}$$

The following identities may be noted which will be used in this work.

- Derivative of a matrix inverse:

$$\frac{\partial \mathbf{K}^{-1}}{\partial \boldsymbol{\theta}} = -\mathbf{K}^{-1}\frac{\partial \mathbf{K}}{\partial \boldsymbol{\theta}}\mathbf{K}^{-1} \tag{21}$$

  where $\frac{\partial \mathbf{K}}{\partial \boldsymbol{\theta}}$ is matrix of element wise derivative.
- Derivative of log determinant of a positive definite symmetric matrix:

$$\frac{\partial \log|\mathbf{K}|}{\partial \boldsymbol{\theta}} = \mathrm{tr}\left(\mathbf{K}^{-1}\frac{\partial \mathbf{K}}{\partial \boldsymbol{\theta}}\right) \tag{22}$$

The double derivative of log likelihood function in Equation 19 with respect to parameter, θ_j, can be succinctly written as

$$\frac{\partial^2 \log p(\mathbf{y}|\mathbf{X})}{\partial \theta_j^2} = -\mathbf{y}^T\left(\mathbf{K}^{-1}\frac{\partial \mathbf{K}}{\partial \theta_j}\right)^2\mathbf{K}^{-1}\mathbf{y} + \frac{1}{2}\mathbf{y}^T\mathbf{K}^{-1}\frac{\partial^2 \mathbf{K}}{\partial \theta_j^2}\mathbf{K}^{-1}\mathbf{y} + \frac{1}{2}\mathrm{tr}\left[\left(\mathbf{K}^{-1}\frac{\partial \mathbf{K}}{\partial \theta_j}\right)^2 - \mathbf{K}^{-1}\frac{\partial^2 \mathbf{K}}{\partial \theta_j^2}\right] \tag{23}$$

Assuming the statistics of $\mathbf{y}$ and then taking the expectation with respect to $\mathbf{y}$ both sides, we get

$$\Rightarrow \mathbb{E}_{\mathbf{y}}\left[\frac{\partial^2 \log p(\mathbf{y}|\mathbf{X})}{\partial \theta_j^2}\right] = -\frac{1}{2}\mathrm{tr}\left[\left(\mathbf{K}^{-1}\frac{\partial \mathbf{K}}{\partial \theta_j}\right)^2\right] \tag{24}$$

On the similar lines, the cross diagonal element of FIM using Equation 19 can be given as

$$\frac{\partial^2 \log p(\mathbf{y}|\mathbf{X})}{\partial \theta_j \partial \theta_k} = -\frac{1}{2}\left[\mathbf{y}^T\mathbf{K}^{-1}\left(\frac{\partial \mathbf{K}}{\partial \theta_k}\mathbf{K}^{-1}\frac{\partial \mathbf{K}}{\partial \theta_j} + \frac{\partial \mathbf{K}}{\partial \theta_j}\mathbf{K}^{-1}\frac{\partial \mathbf{K}}{\partial \theta_k}\right)\mathbf{K}^{-1}\mathbf{y} - \mathbf{y}^T\mathbf{K}^{-1}\frac{\partial^2 \mathbf{K}}{\partial \theta_j \partial \theta_k}\mathbf{K}^{-1}\mathbf{y} - \mathrm{tr}\left(\mathbf{K}^{-1}\frac{\partial \mathbf{K}}{\partial \theta_k}\mathbf{K}^{-1}\frac{\partial \mathbf{K}}{\partial \theta_j} - \mathbf{K}^{-1}\frac{\partial^2 \mathbf{K}}{\partial \theta_j \partial \theta_k}\right)\right] \tag{25}$$

$$\Rightarrow \mathbb{E}_{\mathbf{y}}\left[\frac{\partial^2 \log p(\mathbf{y}|\mathbf{X})}{\partial \theta_j \partial \theta_k}\right] = -\frac{1}{2}\mathrm{tr}\left[\mathbf{K}^{-1}\frac{\partial \mathbf{K}}{\partial \theta_j}\mathbf{K}^{-1}\frac{\partial \mathbf{K}}{\partial \theta_k}\right] \tag{26}$$

In computation of Equation 24 and Equation 26, we require the following derivatives of k with respect to each hyper-parameter using Equation 4.

$$\frac{\partial k}{\partial \sigma_f} = 2\sigma_f \exp\left(-\frac{||\mathbf{x}_i - \mathbf{x}_j||}{2l^2}\right) \tag{27}$$

$$\frac{\partial k}{\partial l} = \frac{\sigma_f^2||\mathbf{x}_i - \mathbf{x}_j||}{l^3}\exp\left(-\frac{||\mathbf{x}_i - \mathbf{x}_j||}{2l^2}\right) \tag{28}$$

Now, substitute Equation 24 and Equation 26 into Equation 13 to get the FIM. To recapitulate, CRLB can be finally given as

$$\mathrm{CRLB}(\boldsymbol{\theta}) \triangleq \sqrt{[\mathbf{I}^{-1}(\boldsymbol{\theta})]_{1,1} + [\mathbf{I}^{-1}(\boldsymbol{\theta})]_{2,2}} = \sqrt{tr(\mathbf{I}^{-1}(\boldsymbol{\theta}))} \tag{29}$$

References

[1] G. Ding, Z. Tan, J. Zhang, L. Zhang, Regional propagation model based fingerprinting localization in indoor environments, in: Personal Indoor and Mobile Radio Communications (PIMRC), 2013 IEEE 24th International Symposium on, IEEE, 2013, pp. 291–295.
[2] T.S. Rappaport, et al., Wireless communications: principles and practice, 2, prentice hall PTR New Jersey, 1996.
[3] C.B. Andrade, R.P.F. Hoefel, IEEE 802.11 WLANs: A comparison on indoor coverage models, in: Electrical and Computer Engineering (CCECE), 2010 23rd Canadian Conference on, IEEE, 2010, pp. 1–6.
[4] A. Borrelli, C. Monti, M. Vari, F. Maz, Channel models for IEEE 802.11 b indoor system design, in: Communications, 2004 IEEE International Conference on, 6, IEEE, 2004, pp. 3701–3705.
[5] B. Ferris, D. Fox, N.D. Lawrence, WiFi-SLAM using gaussian process latent variable models., in: IJCAI, 7, 2007, pp. 2480–2485.

[6] P. Robertson, M. Angermann, M. Khider, Improving simultaneous localization and mapping for pedestrian navigation and automatic mapping of buildings by using online human-based feature labeling, in: Position Location and Navigation Symposium (PLANS), 2010 IEEE/ION, IEEE, 2010a, pp. 365–374.
[7] P. Robertson, M. Angermann, B. Krach, M. Khider, SLAM dance: Inertial-based joint mapping and positioning for pedestrian navigation, Inside GNSS 5 (2010b) 48.
[8] Z. Yang, C. Wu, Y. Liu, Locating in fingerprint space: wireless indoor localization with little human intervention, in: Proceedings of the 18th annual international conference on Mobile computing and networking, ACM, 2012, pp. 269–280.
[9] S. Papaioannou, H. Wen, A. Markham, N. Trigoni, Fusion of radio and camera sensor data for accurate indoor positioning, in: Mobile Ad Hoc and Sensor Systems (MASS), 2014 IEEE 11th International Conference on, IEEE, 2014, pp. 109–117.
[10] H. Wang, S. Sen, A. Elgohary, M. Farid, M. Youssef, R.R. Choudhury, No need to war-drive: unsupervised indoor localization, in: Proceedings of the 10th international conference on Mobile systems, applications, and services, ACM, 2012, pp. 197–210.
[11] G. Shen, Z. Chen, P. Zhang, T. Moscibroda, Y. Zhang, Walkie-markie: Indoor pathway mapping made easy, in: Proceedings of the 10th USENIX conference on Networked Systems Design and Implementation, USENIX Association, 2013, pp. 85–98.
[12] P. Bahl, V.N. Padmanabhan, RADAR: An in-building rf-based user location and tracking system, in: INFOCOM 2000. Nineteenth Annual Joint Conference of the IEEE Computer and Communications Societies. Proceedings, 2, IEEE, 2000, pp. 775–784.
[13] A. LaMarca, Y. Chawathe, S. Consolvo, J. Hightower, I. Smith, J. Scott, T. Sohn, J. Howard, J. Hughes, F. Potter, et al., Place lab: Device positioning using radio beacons in the wild, in: Pervasive computing, Springer, 2005, pp. 116–133.
[14] M. Youssef, A. Agrawala, The horus WLAN location determination system, in: Proceedings of the 3rd international conference on Mobile systems, applications, and services, ACM, 2005, pp. 205–218.
[15] M.B. Kjærgaard, Indoor location fingerprinting with heterogeneous clients, Pervasive and Mobile Computing 7 (1) (2011) 31–43.
[16] S. Yang, P. Dessai, M. Verma, M. Gerla, Freeloc: Calibration-free crowdsourced indoor localization, in: INFOCOM, 2013 Proceedings IEEE, IEEE, 2013, pp. 2481–2489.
[17] C. Laoudias, D. Zeinalipour-Yazti, C.G. Panayiotou, Crowdsourced indoor localization for diverse devices through radiomap fusion, in: Indoor Positioning and Indoor Navigation (IPIN), 2013 International Conference on, IEEE, 2013, pp. 1–7.
[18] Z. Yang, Z. Zhou, Y. Liu, From RSSI to CSI: Indoor localization via channel response, ACM Computing Surveys (CSUR) 46 (2) (2013) 25.
[19] Y. Wen, X. Tian, X. Wang, S. Lu, Fundamental limits of RSS fingerprinting based indoor localization, in: 2015 IEEE Conference on Computer Communications (INFOCOM), IEEE, 2015, pp. 2479–2487.
[20] M. Kotaru, K. Joshi, D. Bharadia, S. Katti, Spotfi: Decimeter level localization using wifi, in: ACM SIGCOMM Computer Communication Review, 45, ACM, 2015, pp. 269–282.
[21] A.T. Mariakakis, S. Sen, J. Lee, K.-H. Kim, SAIL: single access point-based indoor localization, in: Proceedings of the 12th annual international conference on Mobile systems, applications, and services, ACM, 2014, pp. 315–328.
[22] X. Wang, L. Gao, S. Mao, S. Pandey, CSI-based fingerprinting for indoor localization: A deep learning approach, IEEE Transactions on Vehicular Technology (2016), doi:10.1109/TVT.2016.2545523.
[23] Z.-P. Jiang, W. Xi, X. Li, S. Tang, J.-Z. Zhao, J.-S. Han, K. Zhao, Z. Wang, B. Xiao, Communicating is crowdsourcing: Wi-Fi indoor localization with CSI-based speed estimation, Journal of Computer Science and Technology 29 (4) (2014) 589–604.
[24] F. Yu, M. Jiang, J. Liang, X. Qin, M. Hu, T. Peng, X. Hu, 5 G WiFi signal-based indoor localization system using cluster-nearest neighbor algorithm, International Journal of Distributed Sensor Networks 2014 (2014), doi:10.1155/2014/247525.
[25] X. Zhang, Z. Yang, C. Wu, W. Sun, Y. Liu, K. Xing, Robust trajectory estimation for crowdsourcing-based mobile applications, IEEE Transactions on Parallel and Distributed Systems 25 (7) (2014) 1876–1885.
[26] A. Rai, K.K. Chintalapudi, V.N. Padmanabhan, R. Sen, Zee: zero-effort crowdsourcing for indoor localization, in: Proceedings of the 18th annual international conference on Mobile computing and networking, ACM, 2012, pp. 293–304.
[27] M. Alzantot, M. Youssef, Crowdinside: automatic construction of indoor floorplans, in: Proceedings of the 20th International Conference on Advances in Geographic Information Systems, ACM, 2012, pp. 99–108.
[28] R. Gao, M. Zhao, T. Ye, F. Ye, Y. Wang, K. Bian, T. Wang, X. Li, Jigsaw: Indoor floor plan reconstruction via mobile crowdsensing, in: Proceedings of the 20th annual international conference on Mobile computing and networking, ACM, 2014, pp. 249–260.
[29] Y. Zheng, G. Shen, L. Li, C. Zhao, M. Li, F. Zhao, Travi-navi: Self-deployable indoor navigation system, in: Proceedings of the 20th annual international conference on Mobile computing and networking, ACM, 2014, pp. 471–482.
[30] J. Yang, Y. Chen, Indoor localization using improved RSS-based lateration methods, in: Global Telecommunications Conference, 2009. GLOBECOM 2009. IEEE, IEEE, 2009, pp. 1–6.
[31] M. Jadaliha, Y. Xu, J. Choi, N.S. Johnson, W. Li, Gaussian process regression for sensor networks under localization uncertainty, Signal Processing, IEEE Transactions on 61 (2) (2013) 223–237.
[32] J. Medvesek, A. Symington, A. Trost, S. Hailes, Gaussian process inference approximation for indoor pedestrian localisation, Electronics Letters 51 (5) (2015) 417–419.
[33] A. Krause, A. Singh, C. Guestrin, Near-optimal sensor placements in gaussian processes: Theory, efficient algorithms and empirical studies, The Journal of Machine Learning Research 9 (2008) 235–284.
[34] S. Yiu, K. Yang, Gaussian process assisted fingerprinting localization, Internet of Things Journal, IEEE PP (99) (2015), doi:10.1109/JIOT.2015.2481932. 1–1
[35] A. Bekkali, T. Masuo, T. Tominaga, N. Nakamoto, H. Ban, Gaussian processes for learning-based indoor localization, in: Signal Processing, Communications and Computing (ICSPCC), 2011 IEEE International Conference on, 2011, pp. 1–6.
[36] C.E. Rasmussen, C.K.I. Williams, Gaussian processes for machine learning, The MIT Press, 2006.
[37] M. Ebden, Gaussian processes for regression: A quick introduction, The Website of Robotics Research Group in Department on Engineering Science, University of Oxford (2008).
[38] T.F. Coleman, Y. Li, An interior trust region approach for nonlinear minimization subject to bounds, SIAM Journal on optimization 6 (2) (1996) 418–445.
[39] T. Coleman, Y. Li, On the convergence of reflective newton methods for large-scale nonlinear minimization subject to bounds vol. 67, Ithaca, NY, USA: Cornell University (1994).
[40] M.K. Steven, Fundamentals of statistical signal processing, PTR Prentice-Hall, Englewood Cliffs, NJ, 1993.
[41] H.L. Van Trees, Detection, estimation, and modulation theory, optimum array processing, John Wiley & Sons, 2004.
[42] K. Chintalapudi, A. Padmanabha Iyer, V.N. Padmanabhan, Indoor localization without the pain, in: Proceedings of the sixteenth annual international conference on Mobile computing and networking, ACM, 2010, pp. 173–184.
[43] M. Pajovic, P. Orlik, T. Koike-Akino, K.J. Kim, H. Aikawa, T. Hori, An unsupervised indoor localization method based on received signal strength (rss) measurements, in: 2015 IEEE Global Communications Conference (GLOBECOM), IEEE, 2015, pp. 1–6.

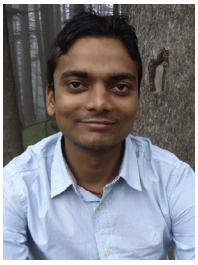

Sudhir Kumar is an Assistant Professor at Visvesvaraya National Institute of Technology (VNIT), Nagpur, India. Prior to this, he worked as a Scientist at TCS Research Kolkata, India. He has also worked with Sensor Networks lab at Department of Computer Science, University of Oxford, United Kingdom as an Erasmus Mundus fellow. He received his B.Tech. degree in Electronics and Communication engineering from West Bengal University of Technology, Kolkata, India in 2010. He obtained his PhD degree at the Department of Electrical Engineering, Indian Institute of Technology Kanpur, India in 2015. He was also a TCS research fellow affiliated to the wireless sensor networks lab at IIT Kanpur. His broad research interest includes wireless sensor networks, cyber-physical systems, internet-of-things (IoT) and pervasive mobile computing. In particular, he works on various applications of signal processing, machine learning and data mining like indoor localization, vehicular tracking, health-care data analytics, and sensor node fault detection.

Rajesh M. Hegde is a Professor in the Department of Electrical Engineering at Indian Institute of Technology Kanpur. His current areas of research interest include multimedia signal processing, multi-microphone speech processing, pervasive multimedia computing, ICT for socially relevant applications in the Indian context, and applications of signal processing in wireless networks with specific focus on emergency response and transportation applications. He has also worked on NSF funded projects on ICT and mobile applications at the University of California San Diego, USA, where he was a researcher and lecturer in the Department of Electrical and Computer Engineering between 2005-2008. He is also a member of the National working group of ITU-T (NWG-16) on developing multimedia applications. Additional biographic information can be found at the URL: http://home.iitk.ac.in/~rhegde.

Niki Trigoni is a Professor at the Department of Computer Science, University of Oxford. She obtained her PhD at the University of Cambridge (2001), became a postdoctoral researcher at Cornell University (2002-2004), and a Lecturer at Birkbeck College (2004-2007). Since she moved to Oxford in 2007, she established the Sensor Networks Group, and has conducted research in communication, localization and in-network processing algorithms for sensor networks. Her recent and ongoing projects span a wide variety of sensor networks applications, including indoor/underground localization, wildlife sensing, road traffic monitoring, autonomous (aerial and ground) vehicles, and sensor networks for industrial processes.